

# Structurally Diverse New Metabolites from Three Hadal Trench-Derived Microorganisms

Qingyun Peng, Wenjia Huang, Xiao Zhang, Xiaoyan Pang, Yunan Liu, Wu Ruan, Qun Li, Li Ding, Huizi Jin, Dehua Yang, Junfeng Wang, and Ming-Wei Wang\*



Cite This: *ACS Omega* 2025, 10, 6201–6209



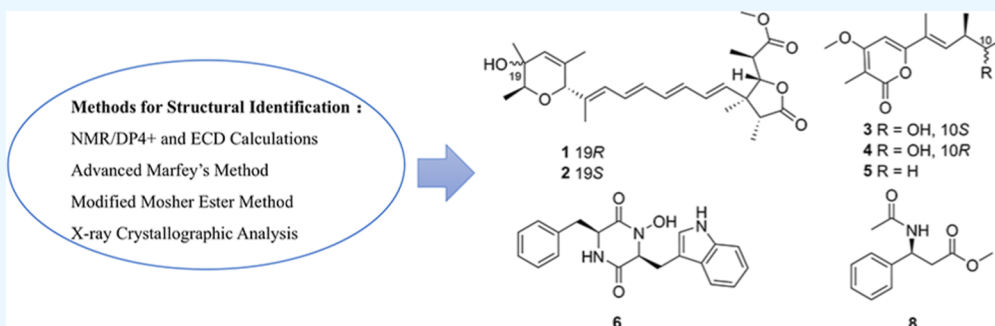
Read Online

ACCESS |

Metrics & More

Article Recommendations

Supporting Information



**ABSTRACT:** Two new tetraene lactone derivatives (**1** and **2**), two new  $\alpha$ -pyrone derivatives (**3** and **4**), three compounds reported as natural products for the first time [an  $\alpha$ -pyrone derivative (**5**), an indole-diketopiperazine alkaloid (**6**), and a  $\beta$ -amino acid derivative (**8**)], and 11 known compounds (**7**, **9–18**), were obtained from microorganisms isolated from hadal trench sediments in the Pacific Ocean. Their structures were determined using NMR, HRESIMS, optical rotatory dispersion (ORD) spectra, NMR calculations followed by DP4+ analysis, electronic circular dichroism (ECD) calculations, X-ray crystallography analysis, and advanced Marfey's and modified Mosher ester methods. Microbial broth dilution assay suggested that compounds **6–11** and **15** had weak antibacterial effects.

## INTRODUCTION

The microbial communities from deepsea environments are adapted to extreme conditions, such as high salinity, high pressure, low temperature, low nutrients, and co-occurring relationships.<sup>1</sup> This is especially true in the hadal trench, where conditions are extremely harsh. Microorganisms living in this zone have created unique metabolic patterns and metabolites through long-term evolution.<sup>2</sup> With significant advances in deepsea sampling techniques and molecular biology tools, increased attention has been paid to the potential applications of deepsea microorganisms and their secondary metabolites in drug discovery and biotechnology.<sup>3</sup> In recent years, notable progress has been made in studying secondary metabolites produced by deepsea microorganisms, especially for antibiotics, anticancer, antifungal, and antiviral substances. Due to the extreme nature of the deepsea environment, these compounds often exhibit complex structures and unique biological activities, presenting significant opportunities to discover novel drug candidates.<sup>4–6</sup> For example, bacteria and fungi isolated from hadal trench environments, such as the Mariana Trench, have been shown to produce compounds with a wide range of pharmacological properties, including antimicrobial, anticancer, antioxidant, and anti-inflammatory activities.<sup>5</sup>

This study aimed to identify new bioactive secondary metabolites produced by hadal trench-derived microorganisms under laboratory conditions. Two fungus, *Penicillium* sp. RCDB001 and *Apiospora* sp. RCDB002, were isolated from the Mariana Trench sediments, and one actinomycete, *Streptomyces* sp. RCDB003, was obtained from the Yap Trench sediments in the Pacific Ocean. A total of 18 compounds were obtained through large-scale fermentation, extraction, and chromatographic isolation, including two new tetraene lactone derivatives (**1** and **2**), two new  $\alpha$ -pyrone derivatives (**3** and **4**), and three compounds reported as natural products for the first time [an  $\alpha$ -pyrone derivative (**5**), an indole-diketopiperazine alkaloid (**6**) and a  $\beta$ -amino acid derivative (**8**)], along with 11 known compounds (**7**, **9–18**). Their antimicrobial activity was assessed using the broth microdilution method. The results showed that compound **15** exhibited weak inhibitory activity

**Received:** December 11, 2024

**Revised:** January 24, 2025

**Accepted:** January 30, 2025

**Published:** February 5, 2025



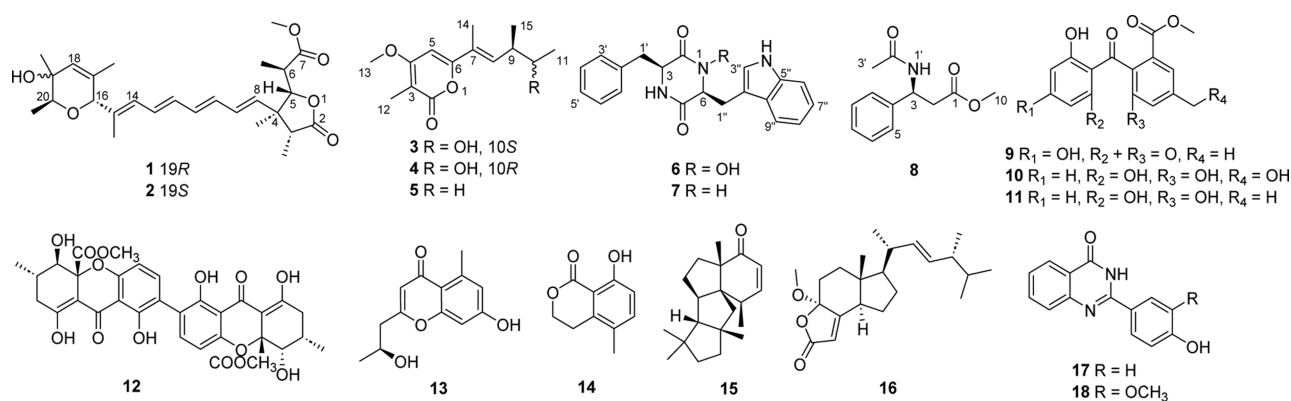


Figure 1. Chemical structures of compounds 1–18.

Table 1. <sup>1</sup>H NMR (600 MHz) and <sup>13</sup>C NMR (150 MHz) Data for Compounds 1 and 2

position	1 <sup>a</sup>		2 <sup>a</sup>		2 <sup>b</sup>	
	δ <sub>C</sub> , type	δ <sub>H</sub> (J in Hz)	δ <sub>C</sub> , type	δ <sub>H</sub> (J in Hz)	δ <sub>C</sub> , type	δ <sub>H</sub> (J in Hz)
1						
2	179.0, C		179.0, C		176.7, C	
3	47.9, CH	2.82, q (7.2)	47.9, CH	2.82, q (7.2)	47.4, CH	2.59, q (7.2)
4	49.6, C		49.6, C		48.4, C	
5	87.2, CH	4.42, d (10.8)	87.2, CH	4.42, d (10.8)	85.7, CH	4.36, d (10.8)
6	42.4, CH	2.77, m	42.4, CH	2.77, m	41.2, CH	2.75, m
7	175.9, C		175.9, C		174.3, C	
8	137.3, CH	5.81, d (14.4)	137.4, CH	5.81, brd (14.4)	136.1, CH	5.67, d (15.0)
9	132.4, CH	6.30, overlapped	132.4, CH	6.27, overlapped	131.1, CH	6.17, overlapped
10	133.5, CH	6.32, overlapped	133.6, CH	6.29, overlapped	132.0, CH	6.24, overlapped
11	134.9, CH	6.41, dd (14.4, 10.8)	134.9, CH	6.38, m	133.7, CH	6.33, dd (14.4, 10.8)
12	134.8, CH	6.33, overlapped	134.7, CH	6.32, overlapped	133.3, CH	6.26, overlapped
13	130.2, CH	6.56, dd (15.0, 11.4)	130.1, CH	6.54, overlapped	129.6, CH	6.50, dd (15.0, 11.4)
14	130.8, CH	6.03, brd (11.4)	130.5, CH	5.91, brd (10.8)	128.9, CH	5.83, d (10.8)
15	136.2, C		135.7, C		135.1, C	
16	81.9, CH	4.28, s	81.6, CH	4.33, s	80.9, CH	4.30, s
17	134.3, C		135.8, C		135.1, C	
18	132.4, CH	5.58, brs	130.9, CH	5.60, brs	130.9, CH	5.66, brs
19	69.8, C		68.1, C		67.4, C	
20	72.6, CH	3.65, q (6.6)	73.2, CH	3.55, q (4.8)	71.2, CH	3.51, q (6.0)
3-CH <sub>3</sub>	7.6, CH <sub>3</sub>	0.97, d (7.2)	7.6, CH <sub>3</sub>	0.97, d (7.2)	7.5, CH <sub>3</sub>	1.02, d (7.2)
4-CH <sub>3</sub>	11.9, CH <sub>3</sub>	1.05, s	11.9, CH <sub>3</sub>	1.05, s	11.8, CH <sub>3</sub>	1.05, s
6-CH <sub>3</sub>	14.2, CH <sub>3</sub>	1.09, d (6.6)	14.2, CH <sub>3</sub>	1.09, d (7.2)	14.0, CH <sub>3</sub>	1.08, d (6.6)
7-OCH <sub>3</sub>	52.5, CH <sub>3</sub>	3.71, s	52.5, CH <sub>3</sub>	3.71, s	52.3, CH <sub>3</sub>	3.72, s
15-CH <sub>3</sub>	15.7, CH <sub>3</sub>	1.88, d (1.2)	15.6, CH <sub>3</sub>	1.86, brs	16.3, CH <sub>3</sub>	1.90, s
17-CH <sub>3</sub>	19.9, CH <sub>3</sub>	1.58, brs	20.1, CH <sub>3</sub>	1.62, brs	20.2, CH <sub>3</sub>	1.63, s
19-CH <sub>3</sub>	22.1, CH <sub>3</sub>	1.11, s	25.6, CH <sub>3</sub>	1.14, s	23.9, CH <sub>3</sub>	1.13, s
20-CH <sub>3</sub>	14.7, CH <sub>3</sub>	1.10, d (6.6)	14.4, CH <sub>3</sub>	1.15, d (4.8)	14.2, CH <sub>3</sub>	1.15, d (6.0)
19-OH		4.51 <sup>c</sup> , s		4.33 <sup>c</sup> , s		

<sup>a</sup>Recorded in CD<sub>3</sub>OD. <sup>b</sup>Recorded in CDCl<sub>3</sub>. <sup>c</sup>Recorded in DMSO-*d*<sub>6</sub>.

against *Enterococcus faecium* RCDB-00011 with a minimum inhibitory concentration (MIC) of 16 μg/mL. In addition, compounds 6–10 and 15 displayed varying degrees of antimicrobial activities against *E. faecium* RCDB-00020, with MIC values of 32 μg/mL for compounds 6 and 8–10, and 16 μg/mL for compounds 7 and 15. Similarly, compounds 9, 11, and 15 showed weak antimicrobial activity against *E. faecium* RCDB-00030 with MIC values of 32 μg/mL.

These findings suggest that microorganisms from deepsea, particularly those from the hadal trench, have the potential to produce structurally diverse and biologically active secondary metabolites. The antimicrobial compounds identified in this

study imply that these microorganisms could serve as valuable resources for drug discovery.<sup>6</sup> Further assessment and characterization of these bioactive metabolites are necessary to explore their therapeutic potential fully.

## RESULTS AND DISCUSSION

Three microorganisms (*Penicillium* sp. RCDB001, *Apiospora* sp. RCDB002 and *Streptomyces* sp. RCDB003) were all cultured on solid medium and extracted with ethyl acetate (EtOAc). The resulting crude extracts were fractionated using a silica gel column and subsequently subjected to high performance liquid chromatography (HPLC) to afford 18

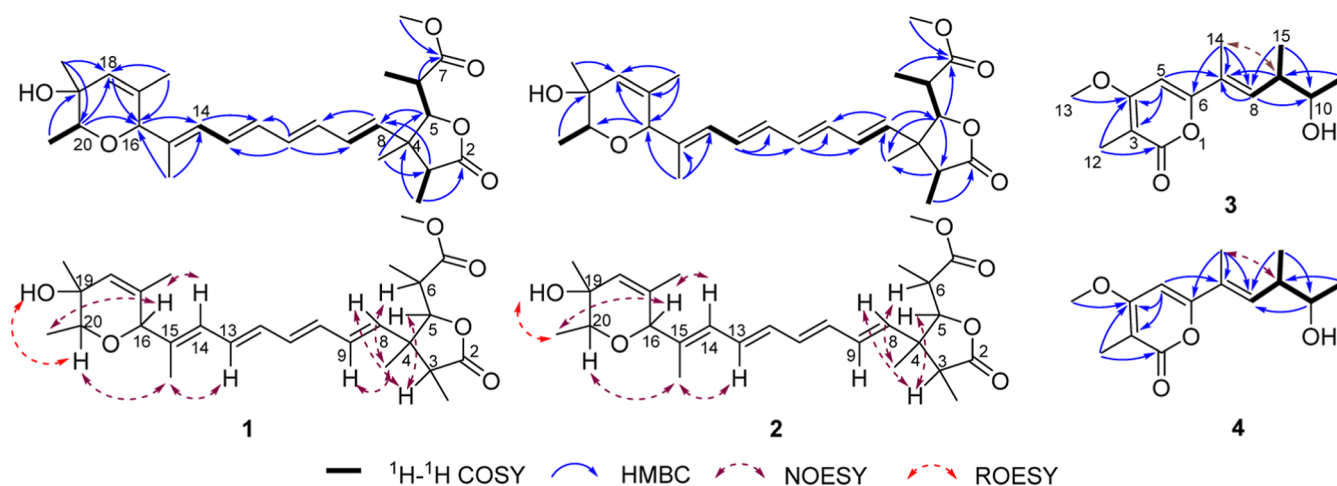


**Figure 2.** Key  $^1\text{H}$ – $^1\text{H}$  COSY, HMBC, NOESY and ROESY correlations of compounds **1**–**4**.  $^1\text{H}$ – $^1\text{H}$  COSY, HMBC and NOESY correlations were observed in  $\text{CD}_3\text{OD}$ , and ROESY correlations were observed in  $\text{DMSO}-d_6$ .

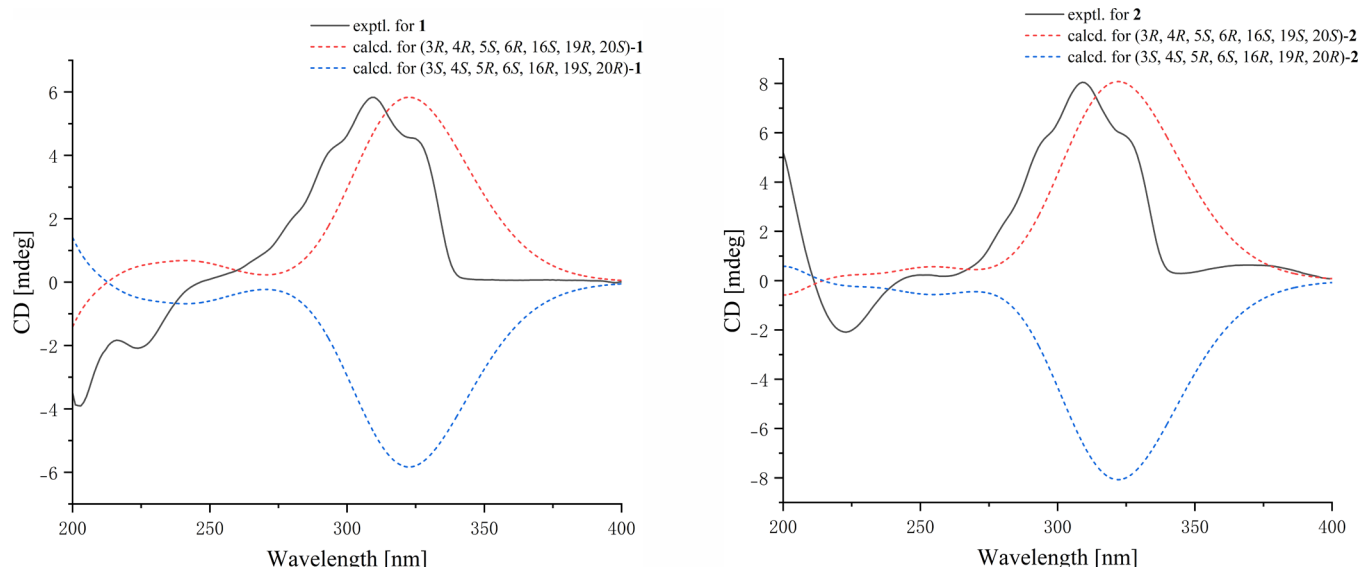


**Figure 3.** Experimental and calculated ECD curves of compounds **1** and **2**.

compounds (**Figure 1**). Two new tetraene lactone derivatives, prugosenes **D** (**1**) and **E** (**2**), together with two new natural products (3*S*,6*S*)-6-((1*H*-indol-3-yl)methyl)-3-benzyl-1-hydroxypiperazine-2,5-dione (**6**) and methyl(*S*)-3-acetamido-3-phenylpropanoate (**8**), were isolated from *Penicillium* sp. RCDB001. Two new  $\alpha$ -pyrone derivatives, alterpyrones **J** (**3**) and **K** (**4**), along with a new natural product (*S*)-aplysiopsene **D** (**5**), were obtained from *Apiospora* sp. RCDB002.

Compound **1** was isolated as a yellow oil. The molecular formula was deduced as  $\text{C}_{27}\text{H}_{38}\text{O}_6$  based on the (+)-HRESIMS ion at  $m/z$  481.2566 [ $\text{M} + \text{Na}$ ] $^+$  (calcd for  $\text{C}_{27}\text{H}_{38}\text{O}_6\text{Na}$ , 481.2561), indicating nine degrees of unsaturation. The  $^1\text{H}$ ,  $^{13}\text{C}$  NMR (**Table 1**), DEPT and HSQC spectra revealed the presence of two ester carbonyls ( $\delta_{\text{C}}$  179.0, C-2; 175.9, C-7), five olefinic bonds ( $\delta_{\text{C}}$  130.2–137.3) (including eight hydrogen-bearing carbons), two  $\text{sp}^3$  quaternary carbons ( $\delta_{\text{C}}$  49.6, C-4; 69.8, C-19), five  $\text{sp}^3$  methines [including three oxygenated methines ( $\delta_{\text{C}/\text{H}}$  87.2/4.42, C-5; 81.9/4.28, C-16; 72.6/3.65, C-20)] and eight methyls [including one oxygenated methyl ( $\delta_{\text{C}/\text{H}}$  52.5/3.71, 7-OCH $_3$ )]. These data showed a close similarity to those reported for prugosene **B2** isolated from

*Penicillium rugulosum*,<sup>7</sup> and then **1** was inferred to be an analogue. Detailed analysis of 1D NMR (**Table 1**), HSQC, HMBC and  $^1\text{H}$ – $^1\text{H}$  COSY spectra (**Figure 2**) revealed that the major difference was the presence of a tetraene chain in **1**, instead of the pentaene chain in prugosene **B2**, which were confirmed by the HMBC correlations from H-3 and H-5 to C-8, from H-8 to C-10, from H-11 to C-9 and C-13, from H-14 to C-12, from 15-CH $_3$  to C-14 and C-16, and from H-16 to C-14. The proton–proton spin-coupling constants ( $^3J_{\text{H8-H9}}$  = 14.4 Hz,  $^3J_{\text{H10-H11}}$  = 14.4 Hz,  $^3J_{\text{H12-H13}}$  = 15.0 Hz) (**Table 1**) and the NOESY correlation between H-13 and 15-CH $_3$  demonstrated that all double bonds possessed an *E*-geometry. Thus, the planar structure of **1** was established as shown (**Figure 1**) and named as prugosene **D**.

The relative configurations at C-3, C-4, C-5, C-16, C-19 and C-20 were established based on NOESY and ROESY correlations (**Figure 2**). The NOESY correlations of H-3/H-5, H-3/H-8, 4-CH $_3$ /H-6, 4-CH $_3$ /H-9, H-14/H-16, H-16/20-CH $_3$ , 15-CH $_3$ /H-20 and the ROESY correlation (**Figure 2**) of 19-OH/H-20 suggested the relative configurations as 3*R*\*, 4*R*\*, 5*S*\*, 16*S*\*, 19*R*\* and 20*S*\*. The relative configuration at

Table 2.  $^1\text{H}$  NMR (600 MHz) and  $^{13}\text{C}$  NMR (150 MHz) Data for Compounds 3–5

position	3 <sup>a</sup>		4 <sup>a</sup>		5 <sup>a</sup>	
	$\delta_{\text{C}}$ , type	$\delta_{\text{H}}$ (J in Hz)	$\delta_{\text{C}}$ , type	$\delta_{\text{H}}$ (J in Hz)	$\delta_{\text{C}}$ , type	$\delta_{\text{H}}$ (J in Hz)
1						
2	167.4, C		167.4, C		167.5, C	
3	102.1, C		102.2, C		102.1, C	
4	169.1, C		169.1, C		168.4, C	
5	94.1, CH	6.50, s	94.2, CH	6.49, s	94.0, CH	6.46, s
6	161.8, C		161.6, C		161.8, C	
7	128.2, C		127.7, C		126.8, C	
8	138.6, CH	6.52, brd (10.8)	138.5, CH	6.44, brd (10.2)	142.1, CH	6.36, d (9.6)
9	41.7, CH	2.64, m	42.1, CH	2.61, m	36.1, CH	2.55, m
10	72.1, CH	3.71, m	72.3, CH	3.64, m	31.1, CH <sub>2</sub>	1.49, m
						1.38, m
11	20.9, CH <sub>3</sub>	1.16, d (6.6)	21.2, CH <sub>3</sub>	1.15, d (6.0)	12.3, CH <sub>3</sub>	0.90, t (7.8)
12	8.5, CH <sub>3</sub>	1.89, s	8.5, CH <sub>3</sub>	1.89, s	8.5, CH <sub>3</sub>	1.89, s
13	57.2, CH <sub>3</sub>	3.99, s	57.3, CH <sub>3</sub>	3.99, s	57.2, CH <sub>3</sub>	3.99, s
14	12.9, CH <sub>3</sub>	1.98, d (1.2)	12.9, CH <sub>3</sub>	1.99, d (1.2)	12.7, CH <sub>3</sub>	1.97, s
15	16.8, CH <sub>3</sub>	1.06, d (6.6)	16.6, CH <sub>3</sub>	1.08, d (6.6)	20.4, CH <sub>3</sub>	1.05, d (6.6)

<sup>a</sup>Recorded in CD<sub>3</sub>OD.

C-6 was determined by NMR calculations followed by DP4+ analysis.<sup>8,9</sup> The  $^{13}\text{C}$  NMR chemical shifts of (3R, 4R, 5S, 6R, 16S, 19R, 20S)-1 and (3R, 4R, 5S, 6S, 16S, 19R, 20S)-1 were calculated by means of the GIAO method at the B3LYP6-31G(d,p) level. The DP4+ probability calculation (Table S1) was subsequently used to compare the theoretical chemical shifts with the experimental values, which confirmed that 3R\*, 4R\*, 5S\*, 6R\*, 16S\*, 19R\*, 20S\* was the most likely relative configuration, with a 100.00% DP4+ probability (Table S1). The theoretical ECD curves of (3R, 4R, 5S, 6R, 16S, 19R, 20S)-1 and (3S, 4S, 5R, 6S, 16R, 19S, 20R)-1 were then calculated and compared with the experimental ECD curve. The latter showed a higher similarity to the calculated ECD curve for (3R, 4R, 5S, 6R, 16S, 19R, 20S)-1 (Figure 3). Accordingly, the absolute configuration of 1 was identified as 3R, 4R, 5S, 6R, 16S, 19R, 20S (Figure 1).

Compound 2 was obtained as a yellow oil with the same molecular formula as that of 1 according to (+)-HRESIMS data, implying nine degrees of unsaturation. The  $^1\text{H}$ ,  $^{13}\text{C}$  NMR (Table 1) and DEPT data of 2 closely resembled those of 1. The major difference was that the chemical shift of methyl group ( $\delta_{\text{C}}$  25.6, recorded in CD<sub>3</sub>OD) attached to C-19 in 2 was downfield shifted with respect to 1 ( $\delta_{\text{C}}$  22.1, recorded in CD<sub>3</sub>OD). In addition, differences in NOESY and ROESY correlations (Figure 2) between 19-OH, H-20 and 20-CH<sub>3</sub> were additionally observed, indicating that the relative configuration of 2 at C-19 was different from that of 1. According to the 1D and 2D NMR data (Table 1 and Figure 2), the planar structure of 2 was established, and the compound was designated as prugosene E.

The NOESY correlations (Figure 2) between H-3/H-5, H-3/H-8, 4-CH<sub>3</sub>/H-6, H-14/H-16, H-16/20-CH<sub>3</sub> and 15-CH<sub>3</sub>/H-20, as well as the ROESY correlation between 19-OH/20-CH<sub>3</sub> (Figure 2), showed the relative configurations as 3R\*, 4R\*, 5S\*, 16S\*, 19S\* and 20S\*. The chemical shifts (recorded in CD<sub>3</sub>OD) of the fragment around the  $\gamma$ -butyrolactone moiety were almost identical to those in 1, suggesting that 2 possessed the same relative configurations as 1 at C-3, C-4, C-5 and C-6. The theoretical ECD curves of (3R, 4R, 5S, 6R, 16S, 19S, 20S)-2 and (3S, 4S, 5R, 6S, 16R, 19R, 20R)-2 were then calculated and compared with the experimental ECD curve

(Figure 3), which assigned the absolute configuration as 3R, 4R, 5S, 6R, 16S, 19S, 20S (Figure 1).

Compound 3 was isolated as a white powder. Its molecular formula was established as C<sub>14</sub>H<sub>20</sub>O<sub>4</sub> based on the (+)-HRESIMS ion at  $m/z$  275.1257 [M + Na]<sup>+</sup> (calcd for C<sub>14</sub>H<sub>20</sub>O<sub>4</sub>Na, 275.1254), accounting for five degrees of unsaturation. The  $^1\text{H}$ ,  $^{13}\text{C}$  NMR (Table 2), DEPT, and HSQC spectra indicated the presence of 14 carbon signals, which accounted for five quaternary carbons [including one ester carbonyl carbon ( $\delta_{\text{C}}$  167.4, C-2) and four olefinic quaternary carbons ( $\delta_{\text{C}}$  169.1, C-4; 161.8, C-6; 128.2, C-7; 102.1, C-3)], four methines [including two sp<sup>3</sup> methines ( $\delta_{\text{C/H}}$  138.6/6.52, C-8; 94.1/6.50, C-5) and one oxygenated methine ( $\delta_{\text{C/H}}$  72.1/3.71, C-10)] and five methyls [including one oxygenated methyl ( $\delta_{\text{C/H}}$  57.2/3.99, C-13)]. The HMBC correlations (Figure 2) from H-5 to C-3 and C-4, from H<sub>3</sub>-12 to C-2 and C-4 and from H<sub>3</sub>-13 to C-4 were in agreement with the presence of an  $\alpha$ -pyrone ring moiety. These NMR data were similar to those described for alterpyrone F, isolated from the endophytic fungus *Alternaria brassicicola*,<sup>10</sup> except for the substitution of the hydroxy group at C-3 in alterpyrone F by a hydrogen ( $\delta_{\text{C/H}}$  41.7/2.64, C-9) in 3. This was further confirmed by the HMBC correlations from H-9 to C-7 and H<sub>3</sub>-11 to C-9. The NOESY correlation between H-9 and H<sub>3</sub>-14 revealed that the double bond possessed an *E*-geometry. Finally, the absolute configuration of 3 was confirmed as 9R, 10S by X-ray crystallographic analysis (Figure 4), and the compound was named as alterpyrone J.

Compound 4 was obtained as a white powder with a molecular formula of C<sub>14</sub>H<sub>20</sub>O<sub>4</sub> established by (+)-HRESIMS. Careful comparison of the 1D NMR data of 4 and 3 (Table 2) revealed a high structural similarity except for some differences in the chemical shifts at C-9/C-10/C-11, suggesting 4 was a diastereomer at C-10 of 3. Analysis of their  $^1\text{H}$ – $^1\text{H}$  COSY, HSQC, and HMBC data (Figure 2) further proves that they have the same planar structure.

The configuration at C-10 was determined by a modified Mosher's method.<sup>10,11</sup> The (S)- and (R)-MTPA esters of 4, 4a and 4b, were obtained by acylation of 4 with (R)- and (S)-MTPA-Cl, respectively. According to the rule of a modified Mosher's method, a 10R configuration in 4 was inferred from



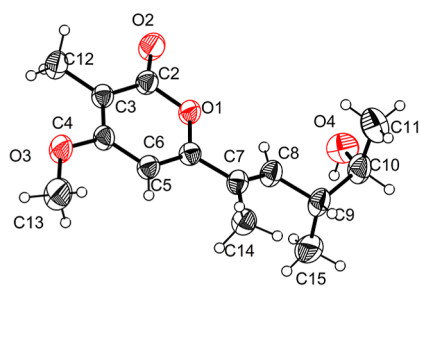


**Figure 4.** Diamond drawing of compound 3 with thermal ellipsoids shown at 50% probability.

the  $\Delta\delta_{\text{H}}$  values ( $\Delta\delta_{\text{H}} = \delta_{\text{S-MTPA-ester}} - \delta_{\text{R-MTPA-ester}}$ ) of the hydrogen signals adjacent to C-10 (Figure 5). Furthermore,

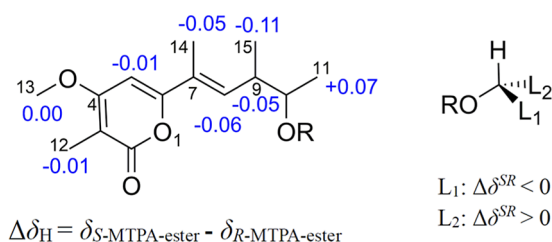


**Figure 5.**  $\Delta\delta_{\text{H(S-R)}}$  (in ppm) values for the MTPA esters of compound 4.

the retention times of 3 and 4 under the same analytical conditions using an ODS column (YMC-pack ODS-A) were different, indicating that 3 and 4 were identified as the epimers at C-10. Thus, the absolute configuration of 4 was established as 9R, 10R (Figure 1).

Compound 5 was isolated as a white powder, and the molecular formula was determined as  $\text{C}_{14}\text{H}_{20}\text{O}_3$  by (+)-HRESIMS. The 1D and 2D NMR data (Table 2 and Figure S1) suggested that 5 possessed the same core molecular skeleton as 3, except for the substitution of the hydroxy group at C-10 in 3 by hydrogen. Based on these data, the structure of 5 was defined, revealing that it possessed the same planar structure as the previously reported compounds (R)- and (S)-aplysiopsene D.<sup>12</sup> Subsequently, the absolute configuration of 5 was identified as 9S (Figure 1) by comparing the ORD data (Supporting Information) with reported compounds. Notably, compound 5 was isolated from a natural source for the first time.<sup>12</sup>

Compound 6 was isolated as a light-yellow powder, with a molecular formula  $\text{C}_{20}\text{H}_{19}\text{N}_3\text{O}_3$  based on (−)-HRESIMS. The 1D and 2D NMR data (Table S2 and Figure S1) showed that it had the same planar structure as a synthesized compound 6-((1*H*-aindol-3-yl)methyl)-3-benzyl-1-hydroxypiperazine-2,5-dione (12a/12b in reference).<sup>13</sup> Compound 6 was transformed from cyclo-(L-tryptophyl-L-phenylalanyl) (7)<sup>14</sup> by oxidation of the amino group (1-NH) to the corresponding hydroxylamine group (1-NOH). The absolute configuration of 7 was determined by the Marfey's method<sup>15</sup> (Figure S2) and X-ray crystallographic analysis (Figure S3), and was finally identified as 3S, 6S. Accordingly, the absolute configuration of 6 at C-3 was inferred as 3S by Marfey's method (Figure S2). The ECD (Figure S4) and ORD data (Supporting Information) of 6 and 7 were subsequently compared to

determine the absolute configuration of 6 at C-6. Thus, 6 was indicated as 3S, 6S (Figure 1), which is also reported as a natural product for the first time.

Compound 8 was obtained as a yellow oil and determined to be  $\text{C}_{12}\text{H}_{15}\text{NO}_3$  based on the (+)-HRESIMS. The planar structure of 8 were indicated as methyl 3-acetamido-3-phenylpropanoate by 1D and 2D NMR spectra (Table S2 and Figure S1). (R)- and (S)-methyl 3-acetamido-3-phenylpropanoate were often synthesized but have never been isolated from natural sources. The absolute configuration of 8 was identified (Figure 1) as 3S by comparing the ORD data (Supporting Information) with synthesized compounds.<sup>16,17</sup>

Eleven known compounds were compared of their spectrometric data with those in the literature and identified as cyclo-(L-tryptophyl-L-phenylalanyl) (7),<sup>14</sup> methyl 6,8-dihydroxy-3-methyl-9-oxo-9*H*-xanthene-1-carboxylate (9),<sup>18</sup> methyl 2-(2,6-dihydroxybenzoyl)-3-hydroxy-5-(hydroxymethyl)benzoate (10),<sup>19</sup> 2,2',6'-trihydroxy-4-methyl-6-methoxy-acyl-diphenylmethanone (11),<sup>20</sup> secalonic acid F (12),<sup>21</sup> (S)-7-hydroxy-2-(2-hydroxypropyl)-5-methyl-4*H*-chromen-4-one (13),<sup>22</sup> 8-hydroxy-5-methylisochroman-1-one (14),<sup>23</sup> conidiogenone B (15),<sup>24</sup> vollemolide (16),<sup>25</sup> 2-(4-hydroxyphenyl)quinazolin-4(3*H*)-one (17)<sup>26,27</sup> and 2-(4-hydroxy-3-methoxyphenyl)quinazolin-4(3*H*)-one (18).<sup>28</sup>

The isolated compounds (3, 5–11, 13 and 15) were assessed for their antibacterial activities against 73 human pathogenic bacteria. Compound 15 showed weak antibacterial effect against *E. faecium* RCDB-00011 with a MIC value of 16  $\mu\text{g/mL}$ . Compounds 6–10 and 15 exhibited weak antibacterial effects against *E. faecium* RCDB-00020 with MIC values of 32, 16, 32, 32, 32, and 16  $\mu\text{g/mL}$ , respectively. Compounds 9, 11, and 15 also displayed weak antibacterial effects against *E. faecium* RCDB-00030 with MIC values of 32  $\mu\text{g/mL}$  (Table S3).

## EXPERIMENTAL SECTION

**General Experiment Procedures.** Optical rotations were taken on a PerkinElmer MPC 500 polarimeter and a Chem Tron P8100 polarimeter. The UV spectra were recorded on an Evolution 350 UV-vis spectrometer. ECD data were measured on a Chirascan V100 spectrometer. The NMR spectra were recorded on Bruker 600 and 800 MHz NMR spectrometers, while HRESIMS data were obtained using Agilent 6520 and 6545 Q-TOF LC-MS spectrometers. Crystal data were obtained on a Bruker D8 Single-Crystal X-ray Diffractometer. The separation and purification of the isolated compounds were carried out using the Agilent 1260 and 1290 HPLC equipped with a 250 mm  $\times$  10 mm i.d., 5  $\mu\text{m}$ , ODS-A column (YMC, Kyoto, Japan). The other semipreparative chromatographic columns used included a 250 mm  $\times$  10 mm i.d., 5  $\mu\text{m}$ , Neptune C18 column (FLM, Guangzhou, China) and a 250 mm  $\times$  10 mm i.d., 5  $\mu\text{m}$ , AZZOTA C18 column (AZZOTA, Delaware and Florida, United States). Medium pressure liquid chromatography (MPLC) separations were performed on a Buchi Sepacore X50 using a C18 column (SW-5222-120-SP, Santai Technologies, Changzhou, China) and glass columns filled with 300–400 mesh silica gel (Qingdao Marine Chemical Factory, Qingdao, China). Thin layer chromatography (TLC) was performed on plates precoated with silica gel GF254 (10–40  $\mu\text{m}$ ) (Qingdao Marine Chemical Factory, Qingdao, China) and spots were detected under 254 nm UV light (WFH-203B, Shanghai Jinke Industrial Co., Ltd., Shanghai, China). The solvents and culture media utilized were sourced from

Sinopharm Chemical Reagent Co., Ltd. (Shanghai, China), while the deuterated solvents were obtained from Cambridge Isotope Laboratories, Inc. (Shanghai, China). Deuterated solvents used for NMR were  $\text{CDCl}_3$  ( $\delta_{\text{H}}$  7.260/ $\delta_{\text{C}}$  77.160),  $\text{CD}_3\text{OD}$  ( $\delta_{\text{H}}$  3.310/ $\delta_{\text{C}}$  49.000) and  $\text{DMSO}-d_6$  ( $\delta_{\text{H}}$  2.500/ $\delta_{\text{C}}$  39.520). FDAA (1-fluoro-2-4-dinitrophenyl-5-L-alanine amide), D- and L-phenylalanine (standards), (R)- and (S)-MTPA-Cl ((S)-(+)-*a*-methoxy-*a*-(trifluoromethyl)-phenylacetyl chloride) were procured from Shanghai Aladdin Biochemical Technology Co., Ltd. (Shanghai, China).

**Microbial Materials and Fermentation.** Of the three microorganisms studied, *Penicillium* sp. RCDB001 and *Apiospora* sp. RCDB002 were isolated from sediments collected at a depth of 9091 m in the Mariana Trench, while *Streptomyces* sp. RCDB003 was isolated from sediments at a depth of 6500 m in the Yap Trench, in the Pacific Ocean. Two fungal strains were identified as *Penicillium* sp. (accession no. PQ329214) and *Apiospora* sp. (accession no. PQ329248) based on ITS region sequences. Additionally, the actinomycete was identified as *Streptomyces* sp. (accession no. PQ345081) based on 16S rRNA region sequences (Supporting Information). Strain RCDB002 was cultured on MB (malt extract powder 15 g, sea salt 15 g,  $\text{H}_2\text{O}$  1 L, agar 15 g, pH 7.4–7.8) agar plates for 3 days before inoculation into MB seed liquid (without agar), which was incubated at 28 °C on a rotary shaker with 180 rpm for 2 days. The seed liquid was then transferred to sterile rice medium (rice 200 g, 3% sea salt water 200 mL, per bottle), and large-scale fermentation was performed in 75 flasks at 25 °C for 31 days. Strain RCDB001 in rich medium (rice 150 g, 1.5% sea salt water 150 mL, per bottle) was fermented similarly in 44 flasks at 25 °C for 31 days under static conditions, while strain RCDB003 in rich medium (rice 150 g, 1.5% sea salt water 150 mL, per bottle) was fermented in 132 flasks at 25 °C for 30 days.

**Extraction and Isolation.** The rice culture of RCDB001 was broken by ultrasonication and transferred to a vat, soaked in 60 L of EtOAc overnight, and the extraction was repeated three times, and the solvent was evaporated to obtain a crude extract (179.1 g), which was subjected to silica gel column chromatography using gradient elution of petroleum ether (PE)–EtOAc (100:1–1:1, v/v, per 10.0 L) and dichloromethane (DCM)–methanol (MeOH) (10:1–5:1, v/v, per 10.0 L), and similar fractions were combined to obtain ten fractions (Fr. A–Fr. J) by observing the spots via TLC. They were separated by MPLC on a C18 column eluting with a gradient of MeOH and  $\text{H}_2\text{O}$  (1:9–1:0, v/v, per 8.0 L) to obtain the corresponding subfractions. Subfraction Fr. B9 was isolated and purified using preparative HPLC with an AZZOTA C18 column (85% ACN in  $\text{H}_2\text{O}$ , v/v, 4 mL/min) to give compound 16 (3.8 mg,  $t_{\text{R}}$  = 29.8 min). Subfraction Fr. C7 was isolated using preparative HPLC with a Neptune C18 column (100% ACN in  $\text{H}_2\text{O}$ , v/v, 2.5 mL/min) to give compound 15 (2.6 mg,  $t_{\text{R}}$  = 24.2 min). Subfraction Fr. D5 was isolated using preparative HPLC with an ODS-A column (54% ACN in  $\text{H}_2\text{O}$ , v/v, 2 mL/min) to give compound 9 (2.2 mg,  $t_{\text{R}}$  = 28.8 min). Subfraction Fr. E6 was separated using preparative HPLC with a Neptune C18 column (75% MeOH in  $\text{H}_2\text{O}$ , v/v, 2 mL/min) to obtain Fr. E6–3, and then the purification of this fraction was continued using HPLC with an ODS-A column (75% MeOH in  $\text{H}_2\text{O}$ , v/v, 2 mL/min) to obtain compound 1 (1.7 mg,  $t_{\text{R}}$  = 30.1 min). Subfraction Fr. F3 was purified using preparative HPLC with a

Neptune C18 column (50% MeOH in  $\text{H}_2\text{O}$ , v/v, 2.5 mL/min) to give compound 11 (5.8 mg,  $t_{\text{R}}$  = 17.0 min). Subfraction Fr. F5 was separated using preparative HPLC with a Neptune C18 column (58% ACN in  $\text{H}_2\text{O}$ , v/v, 3 mL/min) to obtain Fr. F5–3, which was subsequently purified using HPLC with an ODS-A column (75% MeOH in  $\text{H}_2\text{O}$ , v/v, 2 mL/min) to isolate compound 2 (1.6 mg,  $t_{\text{R}}$  = 21.3 min). Pure compound 12 (2.6 mg) was isolated following MPLC. Subfraction Fr. G8 was purified using preparative HPLC with a Neptune C18 column (32% ACN in  $\text{H}_2\text{O}$ , v/v, 2 mL/min) to give compound 10 (7.7 mg,  $t_{\text{R}}$  = 19.0 min). Subfraction Fr. G10 was purified using preparative HPLC with a Neptune C18 column (25% ACN in  $\text{H}_2\text{O}$ , v/v, 3 mL/min) to give compound 8 (8.4 mg,  $t_{\text{R}}$  = 19.0 min). Subfraction Fr. G12 was separated using preparative HPLC with an ODS-A column (27% ACN in  $\text{H}_2\text{O}$ , v/v, 2 mL/min) to obtain Fr. G12–1, which was subsequently purified using HPLC with an ODS-A column (21% ACN in  $\text{H}_2\text{O}$ , v/v, 2 mL/min) to obtain compound 13 (1.6 mg,  $t_{\text{R}}$  = 24.1 min). Subfraction Fr. G14 was purified using preparative HPLC with an ODS-A column (28% ACN in  $\text{H}_2\text{O}$ , v/v, 2 mL/min) to give compound 7 (5.4 mg,  $t_{\text{R}}$  = 32.5 min) and compound 6 (4.9 mg,  $t_{\text{R}}$  = 36.0 min).

The rice culture of RCDB002 was subjected to the same pretreatment to obtain 147.1 g of crude material. The crude material was filtered to remove the spores and insoluble matter and extracted with MeOH and PE three times to obtain the deoiled MeOH extract (75.5 g). The MeOH extract was first partitioned by silica gel column chromatography using gradient of DCM–PE (1:9–1:0, v/v, per 6.0 L) and DCM–MeOH (1:9–1:0, v/v, per 6.0 L) to obtain eight fractions (Fr. 1–Fr. 8). Fr. One (340.4 mg) was separated and purified using analytical HPLC with a Neptune C18 column (43% MeOH in  $\text{H}_2\text{O}$ , v/v, 2 mL/min) to give compound 14 (15.0 mg,  $t_{\text{R}}$  = 9.1 min). Fr. Two (981.6 mg) was separated and purified using preparative HPLC with a Neptune C18 column (80% MeOH in  $\text{H}_2\text{O}$ , v/v, 3 mL/min) to obtain compound 5 (60.0 mg,  $t_{\text{R}}$  = 8.0 min). Fr. Four (698.6 mg) was separated and purified using preparative HPLC with an AZZOTA C18 column (26% ACN in  $\text{H}_2\text{O}$ , v/v, 5 mL/min) to obtain compound 3 (10.0 mg,  $t_{\text{R}}$  = 36.0 min) and compound 4 (4.5 mg,  $t_{\text{R}}$  = 42.0 min).

The rice culture of RCDB003 was subjected to the same pretreatment to obtain 69.3 g of crude material, which was extracted three times with PE and EtOAc after removal of spores and insoluble matter to obtain 41.6 g of EtOAc extract. The EtOAc extract was separated via silica gel column chromatography using gradient elution of PE–EtOAc (10:1–0:1, v/v, per 8.0 L) and EtOAc–MeOH (20:1–0:1, v/v, per 8.0 L), and ten fractions (Fr. 1–Fr. 10) were obtained after TLC spot plate merging. Fr. Four (2.1 g) was subjected to MPLC on a C18 column using an increasing gradient of MeOH– $\text{H}_2\text{O}$  (2:8–1:0, v/v, per 8.0 L). Ten subfractions were obtained, of which, Fr. 4–6 gave compound 17 (4.8 mg,  $t_{\text{R}}$  = 26.0 min) and compound 18 (17.2 mg,  $t_{\text{R}}$  = 28.0 min) by separation of preparative HPLC with an AZZOTA C18 column (9% ACN in  $\text{H}_2\text{O}$ , v/v, 3 mL/min).

**Prugosene D (1).** Yellow oil;  $[\alpha]_{\text{D}}^{25}$  = +97.2 (*c* 0.1, MeOH); UV (MeOH)  $\lambda_{\text{max}}$  (log  $\epsilon$ ) 202 (4.37), 286 (4.30), 298 (4.55), 311 (4.72), 327 (4.67) nm; ECD (0.10 mg/mL, MeOH)  $\lambda_{\text{max}}$  ( $\Delta\epsilon$ ) 216 (–2.55), 224 (–2.89), 310 (+8.10) nm;  $^1\text{H}$  and  $^{13}\text{C}$  NMR data, see Table 1; HRESIMS  $m/z$  481.2566 [ $\text{M} + \text{Na}$ ] $^+$  (calcd for  $\text{C}_{27}\text{H}_{38}\text{O}_6\text{Na}$ , 481.2561).

**Prugosene E (2).** Yellow oil;  $[\alpha]_{\text{D}}^{25}$  = +172.2 (*c* 0.1, MeOH); UV (MeOH)  $\lambda_{\text{max}}$  (log  $\epsilon$ ) 202 (4.22), 286 (4.37), 297 (4.64),

311 (4.82), 327 (4.77) nm; ECD (0.10 mg/mL, MeOH)  $\lambda_{\max}$  ( $\Delta\epsilon$ ) 223 (−2.90), 309 (+11.17), 379 (+0.87) nm;  $^1\text{H}$  and  $^{13}\text{C}$  NMR data, see Table 1; HRESIMS  $m/z$  481.2571  $[\text{M} + \text{Na}]^+$  (calcd for  $\text{C}_{27}\text{H}_{38}\text{O}_6\text{Na}$ , 481.2561).

**Alterpyrone J (3).** White powder;  $[\alpha]_D^{25} = +120.6$  ( $c$  0.1,  $\text{CHCl}_3$ ); UV (MeOH)  $\lambda_{\max}$  ( $\log \epsilon$ ) 229 (4.00), 332 (3.57) nm; ECD (0.10 mg/mL, MeOH)  $\lambda_{\max}$  ( $\Delta\epsilon$ ) 204 (+4.50), 230 (−10.16), 332 (+2.86) nm;  $^1\text{H}$  and  $^{13}\text{C}$  NMR data, see Table 2; HRESIMS  $m/z$  275.1257  $[\text{M} + \text{Na}]^+$  (calcd for  $\text{C}_{14}\text{H}_{20}\text{O}_4\text{Na}$ , 275.1254).

**Alterpyrone K (4).** White powder;  $[\alpha]_D^{25} = +60.1$  ( $c$  0.1,  $\text{CHCl}_3$ ); UV (MeOH)  $\lambda_{\max}$  ( $\log \epsilon$ ) 229 (4.32), 332 (3.91) nm; ECD (0.10 mg/mL, MeOH)  $\lambda_{\max}$  ( $\Delta\epsilon$ ) 204 (+2.75), 230 (−3.72), 335 (+1.27) nm;  $^1\text{H}$  and  $^{13}\text{C}$  NMR data, see Table 2; HRESIMS  $m/z$  253.1439  $[\text{M} + \text{H}]^+$  (calcd for  $\text{C}_{14}\text{H}_{21}\text{O}_4$ , 253.1434).

**X-ray Crystallographic Analysis.** Colorless crystals of compound 3 were obtained in MeOH/ $\text{H}_2\text{O}$  (20:1) solution by slow evaporation at 4 °C. Similarly, colorless crystals of compound 7 were obtained in MeOH/EtOAc (1:2) solution by slow evaporation at room temperature. Their crystals data were collected from a single crystal on a Bruker D8 VENTURE dual wavelength Mo/Cu three-circle diffractometer with a microfocus sealed X-ray tube using mirror optics as a monochromator and a Bruker PHOTON III detector. The crystallographic data of 3 and 7 were measured at 302(2) and 305(2) K, respectively, with Cu  $K_\alpha$  radiation ( $\lambda = 1.54184$  Å). The structure was solved by direct method using SHELXT and refined by full-matrix least-squares approach against  $F^2$  by SHELXL-2019/1.<sup>29,30</sup> All non-hydrogen atoms were refined with anisotropic displacement parameters. All C-bound hydrogen atoms were refined with isotropic displacement parameters. Crystallographic data of 3 and 7 (Tables S4 and S5) have been deposited in the Cambridge Crystallographic Data Centre (deposition number: CCDC 2383472 for 3 and CCDC 2383471 for 7). These data can be obtained, free of charge, on application to CCDC, 12 Union Road, Cambridge CB21EZ, UK [Fax: +44(0)-1223-336033 or E-mail: [deposit@ccdc.cam.ac.uk](mailto:deposit@ccdc.cam.ac.uk)].

**Crystal Data for 3.**  $\text{C}_{14}\text{H}_{20}\text{O}_4$ ,  $M_r = 252.30$ , crystal size  $0.148 \times 0.106 \times 0.040$  mm<sup>3</sup>, monoclinic,  $a = 8.6931(2)$  Å,  $b = 13.3655(3)$  Å,  $c = 12.3407(3)$  Å,  $\alpha = 90^\circ$ ,  $\beta = 110.4850(10)^\circ$ ,  $\gamma = 90^\circ$ ,  $V = 1343.17(5)$  Å<sup>3</sup>,  $T = 302(2)$  K, space group  $P2_1$ ,  $Z = 4$ ,  $\mu(\text{Cu } K_\alpha) = 0.741$  mm<sup>−1</sup>, 27951 reflections collected, 5164 independent reflections ( $R_{\text{int}} = 0.0433$ ,  $R_{\text{sigma}} = 0.0291$ ). The final  $R_1$  values were 0.0338 [ $I \geq 2\sigma(I)$ ]. The final  $wR_2$  values were 0.0924 [ $I \geq 2\sigma(I)$ ]. The final  $R_1$  values were 0.0380 (all data). The final  $wR_2$  values were 0.0946 (all data). The goodness of fit on  $F^2$  was 1.051. The Flack parameter was −0.03(5) (Table S4).

**Crystal Data for 7.**  $\text{C}_{20}\text{H}_{19}\text{N}_3\text{O}_2$ ,  $M_r = 333.38$ , crystal size  $0.267 \times 0.023 \times 0.010$  mm<sup>3</sup>, orthorhombic,  $a = 6.1598(12)$  Å,  $b = 11.719(2)$  Å,  $c = 23.907(5)$  Å,  $\alpha = 90^\circ$ ,  $\beta = 90^\circ$ ,  $\gamma = 90^\circ$ ,  $V = 1725.8(6)$  Å<sup>3</sup>,  $T = 305(2)$  K, space group  $P2_12_12_1$ ,  $Z = 4$ ,  $\mu(\text{Cu } K_\alpha) = 0.681$  mm<sup>−1</sup>, 40646 reflections collected, 3093 independent reflections ( $R_{\text{int}} = 0.0625$ ,  $R_{\text{sigma}} = 0.0232$ ). The final  $R_1$  values were 0.0454 [ $I \geq 2\sigma(I)$ ]. The final  $wR_2$  values were 0.1174 [ $I \geq 2\sigma(I)$ ]. The final  $R_1$  values were 0.0628 (all data). The final  $wR_2$  values were 0.1305 (all data). The goodness of fit on  $F^2$  was 1.036. The Flack parameter was −0.01(11) (Table S5).

**NMR/DP4+ and ECD Calculations.** Conformational analysis of the compounds was conducted via random

searching using Spartan '14 and Gaussian 09 softwares, employing the MMFF94 force field with an energy cutoff of 2.5 kcal/mol for compound 1. The generated conformers were subsequently reoptimized at the B3LYP/6-31G(d,p) level using the TD-DFT method in Gaussian 09. NMR shielding constants in MeOH were calculated in Gaussian 09 using the GIAO method at the B3LYP/6-31G(d,p) level. Boltzmann weights in MeOH were determined using Molclus.<sup>31</sup> The chemical shifts were then applied for DP4+ probability analysis.<sup>8,9</sup> The DP4+ calculation, a computational method that takes into account the distribution of individual chemical shift errors, was performed using a free spreadsheet provided by Nicolás Grimblat and colleagues.<sup>8</sup>

The relative configurations of compounds 1 and 2 also underwent a series of random conformational searches using Spartan '14 software with MMFF94 force field. Subsequently, the low energy conformers were reoptimized using the TD-DFT method at the B3LYP/6-31G(d,p) level in MeOH, employing the IEFPCM model in the Gaussian 09 program. Theoretical calculations for ECD were performed in MeOH at the B3LYP/6-31G(d,p) level. The ECD spectra were generated using Multiwfn,<sup>32</sup> with a half-bandwidth ranging from 0.2 to 0.5 eV, based on the contributions of each conformer calculated via the Boltzmann distribution following UV correction.

#### Preparation of the (S)- and (R)-MTPA Esters of 4.

Compound 4 (0.5 mg), 4-(dimethylamino)pyridine (1.0 mg) and (R)-MTPA-Cl were added to 400  $\mu\text{L}$  stirred pyridine solution. The mixture was reacted at room temperature for 9.0 h and then dried to obtain the reaction product, which was further purified by HPLC with an ODS column (80% MeOH in  $\text{H}_2\text{O}$ , v/v, 3 mL/min) to yield (S)-MTPA ester (4a). The (R)-MTPA ester of 4 (4b) was obtained by following the same experimental procedure.

**(S)-MTPA Ester of 4 (4a).**  $^1\text{H}$  NMR (600 MHz,  $\text{CDCl}_3$ )  $\delta_{\text{H}}$  6.34 (1H, d,  $J = 10.2$  Hz, H-8), 6.11 (1H, s, H-5), 5.07 (1H, m, H-10), 3.90 (3H, s, H<sub>3</sub>-13), 2.79 (1H, m, H-9), 1.94 (3H, s, H<sub>3</sub>-12), 1.84 (3H, s, H<sub>3</sub>-14), 1.32 (3H, d,  $J = 6.6$  Hz, H<sub>3</sub>-11), 0.95 (3H, d,  $J = 6.6$  Hz, H<sub>3</sub>-15).

**(R)-MTPA Ester of 4 (4b).**  $^1\text{H}$  NMR (600 MHz,  $\text{CDCl}_3$ )  $\delta_{\text{H}}$  6.40 (1H, d,  $J = 10.2$  Hz, H-8), 6.12 (1H, s, H-5), 5.05 (1H, m, H-10), 3.90 (3H, s, H<sub>3</sub>-13), 2.84 (1H, m, H-9), 1.95 (3H, s, H<sub>3</sub>-12), 1.89 (3H, s, H<sub>3</sub>-14), 1.25 (3H, d,  $J = 6.6$  Hz, H<sub>3</sub>-11), 1.06 (3H, d,  $J = 6.6$  Hz, H<sub>3</sub>-15).

**Marfey's Analysis.** Compounds 6 and 7 (0.5 mg, each) were respectively hydrolyzed with 1 mL of 6 N HCl at 115 °C for 13.5 h. The hydrolysis product was dried after cooling and dissolved in 100  $\mu\text{L}$  of  $\text{H}_2\text{O}$ . Subsequently, 100  $\mu\text{L}$  of 10 mg/mL FDAA (with acetone as the solvent) and 20  $\mu\text{L}$  of 1 M  $\text{NaHCO}_3$  were added and mixed thoroughly. The derivatization reaction was conducted at 40 °C for 1 h. Following this, 20  $\mu\text{L}$  of 2 M HCl was added to terminate the reaction. The dried mixture was then dissolved in MeOH and analyzed by HPLC with a Neptune C18 column [ACN/( $\text{H}_2\text{O}$  with 0.1% acetic acid) = (15/85–60/40, v/v), 1 mL/min]. The standard amino acids D/L-Phe were subjected to the same derivatization process and HPLC analysis.

**Antibacterial Activities Assay.** The antibacterial activities were determined using the broth microdilution method recommended by the Clinical and Laboratory Standards Institute (CLSI).<sup>33</sup> *Staphylococcus aureus* ATCC 29213, *Escherichia coli* ATCC 25922, *Pseudomonas aeruginosa* 257853 and *Enterococcus faecalis* ATCC 29212 were used as



the quality control strains. A total of 73 pathogenic bacteria were used in the experiment, including nine *Acinetobacter baumannii*, 14 *E. coli* (including five ESBL+, three ESBL- and five carbapenem-resistant strains), 12 *Klebsiella pneumoniae* (including three ESBL+, four ESBL- and five carbapenem-resistant strains), eight *E. faecalis*, nine *S. aureus* (including four methicillin-resistant and four methicillin-sensitive strains), seven *E. faecium*, seven *Stenotrophomonas maltophilia* and seven *P. aeruginosa* (including three carbapenem-resistant and three carbapenem-susceptible). Among them, 69 strains were obtained from clinical isolates.

## ■ ASSOCIATED CONTENT

### ■ Supporting Information

The Supporting Information is available free of charge at <https://pubs.acs.org/doi/10.1021/acsomega.4c11083>.

The 16S rRNA/ITS sequences of strains; the DP4+ analysis data of **1**; the results of the activities assay; the HPLC analysis of Marfey's experiments results; the physicochemical data and key 2D correlations of **5**, **6** and **8**; the UV, NMR and HRESIMS spectra of **1–6**, **8**, and the ECD curves of **6** and **7** (PDF)

X-ray crystallographic data of compound **3** (CIF)

X-ray crystallographic data of compound **7** (CIF)

## ■ AUTHOR INFORMATION

### Corresponding Author

Ming-Wei Wang — Research Center for Deepsea Bioresources, Sanya, Hainan 572025, China; [orcid.org/0000-0001-6550-9017](https://orcid.org/0000-0001-6550-9017); Email: [mwwang@simm.ac.cn](mailto:mwwang@simm.ac.cn)

### Authors

Qingyun Peng — Research Center for Deepsea Bioresources, Sanya, Hainan 572025, China

Wenjia Huang — Research Center for Deepsea Bioresources, Sanya, Hainan 572025, China

Xiao Zhang — School of Pharmaceutical Sciences, Shanghai Jiao Tong University, Shanghai 200240, China

Xiaoyan Pang — South China Sea Institute of Oceanology, Chinese Academy of Sciences, Guangzhou 510301, China

Yunan Liu — Research Center for Deepsea Bioresources, Sanya, Hainan 572025, China

Wu Ruan — Research Center for Deepsea Bioresources, Sanya, Hainan 572025, China

Qun Li — Research Center for Deepsea Bioresources, Sanya, Hainan 572025, China

Li Ding — Institute of Antibiotics, Huashan Hospital, Shanghai Medical College, Fudan University, Shanghai 200040, China

Huizi Jin — School of Pharmaceutical Sciences, Shanghai Jiao Tong University, Shanghai 200240, China; [orcid.org/0000-0002-6901-5898](https://orcid.org/0000-0002-6901-5898)

Dehua Yang — The National Center for Drug Screening, Shanghai 201203, China; [orcid.org/0000-0003-3028-3243](https://orcid.org/0000-0003-3028-3243)

Junfeng Wang — South China Sea Institute of Oceanology, Chinese Academy of Sciences, Guangzhou 510301, China; [orcid.org/0000-0001-8914-5174](https://orcid.org/0000-0001-8914-5174)

Complete contact information is available at: <https://pubs.acs.org/doi/10.1021/acsomega.4c11083>

## Author Contributions

Q.Y.P., W.J.H., X.Z., D.H.Y., and M.-W.W. contributed to the conception and design of the study. Q.Y.P., W.J.H., and X.Z. performed experiments and analyzed data. Q.Y.P. and X.Z. wrote the manuscript. J.F.W. and M.-W.W. edited the manuscript. L.D. performed the antibacterial assay. Y.N.L., W.R., and Q.L. obtained spectral data of the compounds. J.F.W. helped the identification of compounds. All the authors read and approved the submitted version.

## Notes

The authors declare no competing financial interest.

## ■ ACKNOWLEDGMENTS

This work was partially supported by a collaboration grant from Zhejiang Engineering Research Center of Advanced Mass Spectrometry and Clinical Application (no. zyk2204) and Hainan Provincial Major Science and Technology Project (no. ZDKJ2021028). The authors are grateful to W.J. Zhang and Y.H. Liu for their valuable support, and to J.L. She helps with NMR and ECD calculations.

## ■ REFERENCES

- (1) Bhatnagar, I.; Kim, S. K. Immense essence of excellence: marine microbial bioactive compounds. *Mar. Drugs* **2010**, *8*, 2673–2701.
- (2) Xiong, Z. Q.; Wang, J. F.; Hao, Y. Y.; Wang, Y. Recent advances in the discovery and development of marine microbial natural products. *Mar. Drugs* **2013**, *11*, 700–717.
- (3) Feng, J. C.; Liang, J. Z.; Cai, Y. P.; Zhang, S.; Xue, J. C.; Yang, Z. F. Deep-sea organisms research oriented by deep-sea technologies development. *Sci. Bull.* **2022**, *67*, 1802–1816.
- (4) Tortorella, E.; Tedesco, P.; Esposito, F. P.; January, G. G.; Fani, R.; Jaspars, M.; de Pascale, D. Antibiotics from deep-sea microorganisms: current discoveries and perspectives. *Mar. Drugs* **2018**, *16*, 355.
- (5) Kaleem, S.; Qin, L.; Yi, W. W.; Lian, X. Y.; Zhang, Z. Z. Bioactive metabolites from the Mariana Trench sediment-derived fungus *Penicillium* sp. SY2107. *Mar. Drugs* **2020**, *18*, 258.
- (6) Cong, M. J.; Pang, X. Y.; Zhao, K.; Song, Y.; Liu, Y. H.; Wang, J. F. Deep-sea natural products from extreme environments: cold seeps and hydrothermal vents. *Mar. Drugs* **2022**, *20*, 404.
- (7) Lang, G.; Wiese, J.; Schmaljohann, R.; Imhoff, J. F. New pentaenes from the sponge-derived marine fungus *Penicillium rugulosum*: structure determination and biosynthetic studies. *Tetrahedron* **2007**, *63*, 11844–11849.
- (8) Grimblat, N.; Zanardi, M. M.; Sarotti, A. M. Beyond DP4: an improved probability for the stereochemical assignment of isomeric compounds using quantum chemical calculations of NMR shifts. *J. Org. Chem.* **2015**, *80*, 12526–12534.
- (9) Colasurdo, D. D.; Arancibia, L. A.; Naspi, M. L.; Laurella, S. L. Using DP4+ probability for structure elucidation of sesquiterpenic lactones: the case of (–)-istanbulin A. *J. Phys. Org. Chem.* **2022**, *35*, 27–32.
- (10) Li, F. L.; Ye, Z.; Huang, Z. Y.; Chen, X.; Sun, W. G.; Gao, W. X.; Zhang, S.; Cao, F.; Wang, J.; Hu, Z.; et al. New  $\alpha$ -pyrone derivatives with herbicidal activity from the endophytic fungus *Alternaria brassicicola*. *Bioorg. Chem.* **2021**, *117*, 105452.
- (11) Hoyer, T. R.; Jeffrey, C. S.; Shao, F. Mosher ester analysis for the determination of absolute configuration of stereogenic (chiral) carbinol carbons. *Nat. Protoc.* **2007**, *2*, 2451–2458.
- (12) Geiseler, O.; Podlech, J. Total synthesis of infectopyrone, aplysiopsenes A–C, ent-aplysiopene D, phomapyrones A and D, 8,9-dehydroxylarone, and nectriapyrone. *Tetrahedron* **2012**, *68*, 7280–7287.
- (13) Pham, T. L.; Sae-Lao, P.; Toh, H. H. M.; Csókás, D.; Bates, R. W. The total synthesis of raistrickindole A. *J. Org. Chem.* **2022**, *87*, 16111–16114.



- (14) Tan, J. J.; Liu, X. Y.; Yang, Y.; Li, F. H.; Tan, C. H.; Li, Y. M. Aspergillolide, a new 12-membered macrolide from sea cucumber-derived fungus *Aspergillus* sp. S-3-75. *Nat. Prod. Res.* **2020**, *34*, 1131–1137.
- (15) Liang, X.; Nong, X. H.; Huang, Z. H.; Qi, S. H. Antifungal and antiviral cyclic peptides from the deep-sea-derived fungus *Simplicillium obclavatum* EIODSF 020. *J. Agric. Food Chem.* **2017**, *65*, 5114–5121.
- (16) Zhou, Y. G.; Tang, W. J.; Wang, W. B.; Li, W. G.; Zhang, X. M. Highly effective chiral *ortho*-substituted BINAPO ligands (*o*-BINAPO): applications in Ru-catalyzed asymmetric hydrogenations of  $\beta$ -aryl-substituted  $\beta$ -(acylamino)acrylates and  $\beta$ -keto esters. *J. Am. Chem. Soc.* **2002**, *124*, 4952–4953.
- (17) Li, X. X.; You, C.; Li, S. L.; Lv, H.; Zhang, X. M. Nickel-catalyzed enantioselective hydrogenation of  $\beta$ -(acylamino)acrylates: synthesis of chiral  $\beta$ -amino acid derivatives. *Org. Lett.* **2017**, *19*, 5130–5133.
- (18) Jin, Y. Z.; Qin, S. D.; Gao, H.; Zhu, G. L.; Wang, W.; Zhu, W. M.; Wang, Y. An anti-HBV anthraquinone from aciduric fungus *Penicillium* sp. OUCMDZ-4736 under low pH stress. *Extremophiles* **2018**, *22*, 39–45.
- (19) Zhuang, P.; Tang, X. X.; Yi, Z. W.; Qiu, Y. K.; Wu, Z. Two new compounds from marine-derived fungus *Penicillium* sp. F11. *J. Asian Nat. Prod. Res.* **2012**, *14*, 197–203.
- (20) Niu, Z.; Chen, Y. C.; Guo, H.; Li, S. N.; Li, H. H.; Liu, H. X.; Liu, Z. M.; Zhang, W. M. Cytotoxic polyketides from a deep-sea sediment derived fungus *Diaporthe phaseolorum* FS431. *Molecules* **2019**, *24*, 3062.
- (21) Yamazaki, H.; Ukai, K.; Namikoshi, M. Asperdichrome, an unusual dimer of tetrahydroxanthone through an ether bond, with protein tyrosine phosphatase 1B inhibitory activity, from the Okinawan freshwater *Aspergillus* sp. TPU1343. *Tetrahedron Lett.* **2016**, *57*, 732–735.
- (22) Kashiwada, Y.; Nonaka, G.; Nishioka, I. Studies on Rhubarb (*Rhei Rhizoma*). 5. Isolation and characterization of chromone and chromanone derivatives. *Chem. Pharm. Bull.* **1984**, *32*, 3493–3500.
- (23) Huang, C.; Xiong, J.; Guan, H. D.; Wang, C. H.; Lei, X. S.; Hu, J. F. Discovery, synthesis, biological evaluation and molecular docking study of (*R*)-5-methylmellein and its analogs as selective monoamine oxidase A inhibitors. *Bioorg. Med. Chem.* **2019**, *27*, 2027–2040.
- (24) Du, L.; Li, D. H.; Zhu, T. J.; Cai, S. X.; Wang, F. P.; Xiao, X.; Gu, Q. Q. New alkaloids and diterpenes from a deep ocean sediment derived fungus *Penicillium* sp. *Tetrahedron* **2009**, *65*, 1033–1039.
- (25) Kobata, K.; Wada, T.; Hayashi, Y.; Shibata, H. Volemolide, a novel norsterol from the fungus *Lactarius Volemus*. *Biosci., Biotechnol., Biochem.* **1994**, *58*, 1542–1544.
- (26) Xue, J. H.; Xu, L. X.; Jiang, Z. H.; Wei, X. Y. Quinazoline alkaloids from *Streptomyces michiganensis*. *Chem. Nat. Compd.* **2012**, *48*, 839–841.
- (27) Kornsakulkarn, J.; Saepua, S.; Srijomthong, K.; Rachtawee, P.; Thongpanchang, C. Quinazolinone alkaloids from actinomycete *Streptomyces* sp. BCC 21795. *Phytochem. Lett.* **2015**, *12*, 6–8.
- (28) Liu, Y.; Liu, J. S.; Yan, P. C.; Kachanuban, K.; Liu, P. P.; Jia, A. Q.; Zhu, W. M. Carbazole and quinazolinone derivatives from a fluoride-tolerant *Streptomyces* strain OUCMDZ-SS11. *J. Agric. Food Chem.* **2024**, *72*, 6424–6431.
- (29) Sheldrick, G. M. Crystal structure refinement with SHELXL. *Acta Crystallogr., Sect. C: Struct. Chem.* **2015**, *71*, 3–8.
- (30) Sheldrick, G. M. SHELXT—integrated space-group and crystal-structure determination. *Acta Crystallogr., Sect. A: Found. Adv.* **2015**, *71*, 3–8.
- (31) Lu, T. Molclus Program, Version 1.9.9.9, 2022. <http://www.keinsci.com/research/molclus.html> (accessed May 1, 2022).
- (32) Lu, T.; Chen, F. Multiwfn a multifunctional wavefunction analyzer. *J. Comput. Chem.* **2012**, *33*, 580–592.
- (33) Clinical and Laboratory Standards Institute. *Performance Standards for Antimicrobial Susceptibility Testing*; CLSI M100-Ed33: Wayne, PA, 2023.